acta physica slovaca vol. 44 No. 4/5, 403 – 416 August 1994

ELECTRONIC PHASE SEPARATION IN HIGH-T_C SUPERCONDUCTORS[1]

E. Sigmund†, V. Hizhnyakov‡, G. Seibold†
†*Institut f. Physik, Technische Universität Cottbus, POB 101344, 03013 Cottbus, FRG*
‡*Institute of Physics,Estonian Academy of Sciences, Riia 142,Tartu,Estonia*

Received 16 May 1994, accepted

When doping the antiferromagnetically (AF) ordered high-T_c cuprates with holes magnetic polarons (spin-polarized clusters) are formed. We discuss two different mean-field approaches of the three-band Hubbard model to calculate binding energy and polarization of the clusters. At higher hole concentrations and due to cluster diffusion a phase separation is formed by establishing large fractal or percolative clusters. This percolation picture allows to understand experimentally obtained results for phase separation as well as magnetic and conductive phase diagrams.

1. Introduction

Doping or oxydation of the antiferromagnetically (AF) ordered perovskite compounds like La_2CuO_4 and $YBa_2Cu_3O_6$, which are the parent materials for high-T_c superconductors, leads to the creation of holes in the CuO_2 planes. The dynamics of the charge carriers is governed by strong correlation effects which causes a redistribution of spin and charge densities in the vicinity of the excess holes. Due to these effects the antiferromagnetic order in the CuO_2 planes disappears quickly with doping and at higher doping concentrations superconductivity is established below the critical temperature.

A large number of experiments show that upon doping the high-T_c cuprates a separation into small charge carrier enriched domains and carrier depleted regions takes place [1, 2, 3, 4]. The results of these investigations give support to an electronic mechanism of the phase separation in contrast to a chemical phase separation where the excess oxygen ions should cluster in domains. The simultaneous observation of a diamagnetic signal below T_c and a Néel temperature of $T \approx 250K$ in $La_2CuO_{4+\delta}$ samples [1] strongly indicates a separation mechanism of percolative type as proposed in the model of percolative phase separation [5]. This model is based on the idea that doping

[1]Invited lecture at MECO (Middle European CoOperation) 19, Smolenice, Slovakia, April 11-15, 1994

0323-0465/94

of the CuO_2-planes with holes leads to the creation of small ferromagnetically ordered clusters (magnetic polarons, ferrons). These clusters have only low mobility whereas the holes inside the clusters can move freely. As a result, when increasing the hole concentration and due to cluster diffusion the clusters start to overlap and a (fractal) percolation network is built up. This leads to the destruction of the AF order and to the appearance of metallic-like conductivity, or below T_c to superconductivity, within the percolation network [5].

This model allows to explain the phase diagrams of $La_{2-x}Sr_xCuO_4$ and $YBa_2Cu_3O_{6+\delta}$ in quantitative agreement with experiment [6] giving support to spin cluster (magnetic polaron) formation in these materials. The spin cluster model also allows to explain recent experimental data on percolative phase separation in weakly doped $La_2CuO_{4+\delta}$ and $La_{2-x}Sr_xCuO_4$ samples [1, 7]. Also the magnetic susceptibility measurements [1] show the existence of small ferromagnetic (superparamagnetic) particles associated with holes. Recently, the existence of spin-polarized clusters in $La_2CuO_{4+\delta}$ has been demonstrated by EPR [8] and neutron scattering [9] experiments. In addition, magnetic resonance signals measured in $RBa_2Cu_3O_x$ (R=Y,Gd) have been attributed to clusters with magnetic ordering [10]. A review on experiments about phase separation is given in [11, 12].

This paper is organized as follows. After introducing the three-band Hubbard model we calculate the Green's functions in the Hartree-Fock approximation. It is shown that spin-polarized clusters are created upon doping whose polarization, binding energy and effective mass are obtained by a Lifshitz formalism. The influence of fluctuations is investigated within the scope of the slave boson method in the saddle-point approximation. The last two sections are devoted to the percolation mechanism and its experimental evidence.

2. Hole dynamics in CuO_2 planes

Our considerations are based on the three band Hubbard model (see e.g. Emery [13]) which takes the $d_{x^2-y^2}$ band of the Cu ions and the p_σ bands of the oxygen ions into account. The model hamiltonian reads

$$H = \sum_\sigma H_{0\sigma} + H_{int} \tag{1}$$

where

$$H_{0\sigma} = \epsilon_d \sum_n n^d_{n\sigma} + \epsilon_p \sum_m n^p_{m\sigma} + T^{\pm} \sum_{nm} \left(d^\dagger_{n\sigma} p_{m\sigma} + h.c.\right) \tag{2}$$

$$H_{int} = U \sum_n n^d_{n\sigma} n^d_{n-\sigma} \tag{3}$$

$n^d_{n\sigma}$ and $n^p_{m\sigma}$ are the electronic occupation numbers of the $d_{x^2-y^2}$ and p_σ orbitals, respectively, $d^\dagger(d)$ and $p^\dagger(p)$ are electronic creation (annihilation) operators in the corresponding Cu and O orbitals obeying the usual commutation rules for fermion operators. The spin index σ indicates the spin directions ($\sigma = \uparrow\downarrow$). Only the transfer between Cu and the four nearest oxygen ions is taken into account. The transfer integral $T^{\pm}$ changes sign due to the two possibilities of overlap. H_{int} describes the Coulomb repulsion for two electrons on the same Cu site with opposite spins. Band structure calculations indicate the following parameter values: $U \approx 8eV$, $\epsilon = \epsilon_p - \epsilon_d \approx 3eV$, $T \approx 1eV$.

The effect of the strong particle-particle (Hubbard) repulsion is treated by two different approaches.

2.1. Hartree-Fock approach

In our first approach the calculation is based on a Hartree-Fock approximation of the original three-band Hubbard hamiltonian which within this approximation reads as

$$H^{MF} = \sum_\sigma H^{MF}_{0\sigma} + H^{MF}_{int} \tag{4}$$

where

$$H^{MF}_{0\sigma} = \sum_n \left(\epsilon_d + U\langle n^d_{n-\sigma}\rangle\right) n^d_{n\sigma} + \epsilon_p \sum_m n^p_{m\sigma} + T^{\pm} \sum_{nm} \left(d^\dagger_{n\sigma} p_{m\sigma} + h.c.\right) \tag{5}$$

$$H^{MF}_{int} = -U \sum_n \langle n^d_{n\sigma}\rangle \langle n^d_{n-\sigma}\rangle \tag{6}$$

In the AF spin-wave approximation the state vector corresponding to the two different Cu ions in a unit cell are denoted by d_1 and d_2. The corresponding diagonal elements of the hamiltonian (4) read

$$\epsilon_{1\sigma} = \epsilon_d + U\langle n_{1-\sigma}\rangle \tag{7}$$

$$\epsilon_{2\sigma} = \epsilon_d + U\langle n_{2-\sigma}\rangle \tag{8}$$

From the symmetry of the AF state one obtains immediately the following relations

$$\langle n_{1\uparrow}\rangle = \langle n_{2\downarrow}\rangle \tag{9}$$

$$\langle n_{1\downarrow}\rangle = \langle n_{2\uparrow}\rangle \tag{10}$$

Therefore we can use the notations $\langle n_\uparrow\rangle$ and $\langle n_\downarrow\rangle$ and consider these quantities as modulated with twice the lattice period.

Upon transforming (5) into **k**-space one finds that two oxygen-states are decoupled from all other states while in the basis of the four remaining states the hamiltonian (5) reads as

$$H_{\mathbf{kk}} = \begin{pmatrix} \epsilon_1 & 0 & -TV_k & -2T\sqrt{1-\frac{1}{4}V_k^2} \\ 0 & \epsilon_2 & 2T & 0 \\ -TV_k & 2T & \epsilon_p & 0 \\ -2T\sqrt{1-\frac{1}{4}V_k^2} & 0 & 0 & \epsilon_p \end{pmatrix} \tag{11}$$

with $V_k = \cos k_x + \cos k_y$. The secular equation reads

$$Det[E - H_{\mathbf{kk}}] = D_1(E)D_2(E) - 4T^4V_k^2 \tag{12}$$

where

$$D_i(E) = (E - \epsilon_p)(E - \epsilon_i) - 4T^2 \tag{13}$$

Eq. (12) describes four bands where in the case of CuO_2 only the lowest band is filled with holes. A pecular property of the model is the appearance of nonanalytical critical points along the line $k_x + k_y = \pi$. These critical points lead to a divergent behaviour in the density of states of the type $\frac{1}{\sqrt{E}} \ln \frac{1}{E}$, while normal logarithmic singularities disappear.

2.2. Green's Functions

The diagonal elements of the one-particle Green's functions for the two Cu sites in the doubled unit cell are given by

$$G_{ii} = \sum_{\mathbf{k}} (E - H_{\mathbf{kk}})^{-1}_{ii} = \sum_{\mathbf{k}} \frac{|\{E - H_{\mathbf{kk}}\}|_{ii}}{det|E - H_{\mathbf{kk}}|} \tag{14}$$

where $|\{A\}|_{ii}$ denotes the adjoint subdeterminant of elememt (ii) of the matrix A. We define the imaginary part of the complex energy to be negative: $E \rightarrow E - i\epsilon$. Making use of Eqs. (9) and (10) we write the Green's function on Cu site 1 as $G_{11} = G_\uparrow$ and on Cu site 2 as $G_{22} = G_\downarrow$, respectively. After a straightforward calculation one can express G_σ in terms of the Green's function G^{2-D} of a simple quadratic lattice which yields

$$G_\uparrow = (E - \epsilon_p)\sqrt{\frac{D_2}{D_1}} G^{2-D}(\sqrt{D(E)}) \tag{15}$$

$$G_\downarrow = (E - \epsilon_p)\sqrt{\frac{D_1}{D_2}} G^{2-D}(\sqrt{D(E)}) \tag{16}$$

where $D(E) = D_1(E)D_2(E)$. G^{2-D} is derived in [14] and is given by a simple elliptic integral of the first kind **IK**.

In fig.(1) we have plotted the real and imaginary part of $G_\uparrow$ and $G_\downarrow$ up to the second hole band. The expectation values $\langle n_\uparrow \rangle$ and $\langle n_\downarrow \rangle$ are immediately found from the selfconsistent equations

$$\langle n_\uparrow \rangle = \frac{1}{\pi} \int dE\, Im(G_\uparrow(E)) \tag{17}$$

$$\langle n_\downarrow \rangle = \frac{1}{\pi} \int dE\, Im(G_\downarrow(E)) \tag{18}$$

where the integration is restricted to the lowest hole band. As can be seen from table (1), for real values of parameters the ground state is almost completely polarized although the total Cu spin is considerably smaller due to the p-d hybridization. The ground state properties of the totally AF ordered lattice have been intensively discussed in [15].

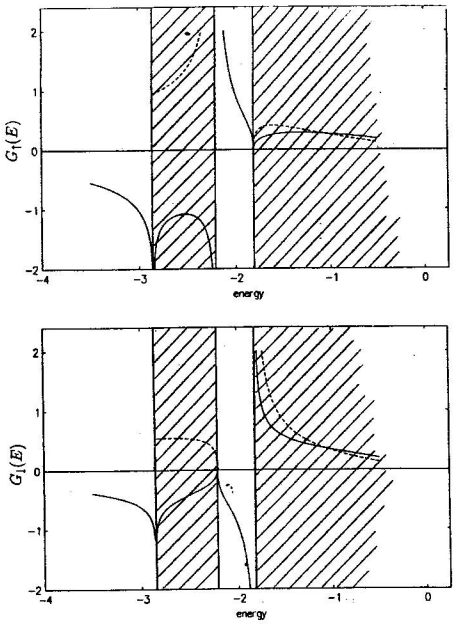

Fig. 1. Local Green functions for spin-up (a) and spin-down (b) projections of the wave-function on Cu sites. The shaded areas indicate the lower Hubbard band and the lower part of the bonding oxygen band. Solid line is real part, dashed line is imaginary part of the Green functions.

2.3. Doped system

When doping the system with holes one can expect (in analogy with e.g. electron-lattice polaron theory) a spontanous symmetry breaking, leading to the creation of localized excitations. The new states arising from such symmetry breaking should be determined selfconsistently.

In the following we assume that the Cu spin at site $\mathbf{m} = 0$, which has originally spin direction, say $\uparrow$, can spontaneously fluctuate, changing the spin values to $\langle n^l_\uparrow \rangle$ and $\langle n^l_\downarrow \rangle$. These values are treated selfconsistently. This problem is mathematically similar to the problem of magnetic impurities (e.g. Wolff model) and can be treated within the standard localized perturbation theory. The perturbation of the hamiltonian (5) is given by

$$V = V^\uparrow + V^\downarrow \tag{19}$$

where

$$V^\downarrow_{mm'} = U\delta_{m0}\delta_{m'0}(\langle n^l_\uparrow \rangle - \langle n_\uparrow \rangle) d^\dagger_{0\downarrow} d_{0\downarrow} \tag{20}$$

$$V^\uparrow_{mm'} = U\delta_{m0}\delta_{m'0}(\langle n^l_\downarrow \rangle - \langle n_\downarrow \rangle) d^\dagger_{0\uparrow} d_{0\uparrow} \tag{21}$$

The new Green's functions for each spin direction can be found from Dyson's equation

$$G^\sigma(mm^l) = G_0^\sigma(mm^l) + G_0^\sigma(m0)V^\sigma G^\sigma(0m^l) \tag{22}$$

where G_0 denotes the Green's function of the undisturbed lattice. The solution of (22) is

$$G^\sigma(mm^l) = G_0^\sigma(mm^l) + V^\sigma \frac{G_0^\sigma(m0)G_0^\sigma(0m^l)}{1 - V^\sigma G_0^\sigma(00)} \tag{23}$$

The equations determining the spin distribution at the disturbed lattice site then read as

$$\langle n_\sigma^l \rangle = \frac{1}{\pi} \int_{-\infty}^{E_F} dE \, Im\, G^\sigma(00, E) \tag{24}$$

where E_F is the chemical potential, depending on the number of additional holes. The localized states are the solution of eqs.

$$1 = V^\sigma G_0^\sigma(E), \quad \sigma = \uparrow, \downarrow \tag{25}$$

As can be concluded from the real part of $G(E)$ in fig.(1), Eq.(25) has only solutions with $V^\uparrow > 0$ and $V^\downarrow < 0$ (beside the trivial solution $V^\sigma = 0$). It is seen for any values of parameters three localized states exist, one originating from the change of the $\langle n_\uparrow \rangle$ value and two due to the perturbation of $\langle n_\downarrow \rangle$. For one additional hole the Fermi level coincides with the upper localized level in the gap.

The total change of energy caused by a spin-flip process is a sum of the energy change in the bands and the contributions of the localized states

$$\Delta E^{loc} = \sum_l E_l + \frac{1}{\pi} \sum_\sigma \int_{E_0}^{E_1} \arctan \frac{V^\sigma Im\, G^\sigma(00)}{1 - V^\sigma Re\, G^\sigma(00)} dE \tag{26}$$

where E_l denote the energies of the occupied localized states measured from the band edges.

The energy change resulting from the perturbation of (6) reads as

$$\Delta E^{int} = U(\langle n_\uparrow \rangle \langle n_\downarrow \rangle - (\langle n_\uparrow^l \rangle \langle n_\downarrow^l \rangle)) \tag{27}$$

2.4. Results

As can be seen from table (1) the formation of a single flip spin polaron yields a remarkably large binding energy which is due to the strong correlations in the system. For a critical value of U the situation with two turned spins (diagonally neighboured) gives a larger binding energy. This behaviour is in agreement with calculations of Auerbach and Larson [16] for the t-J-model. In the mean-field picture two turned spins maximally produce four localized states in the CT-gap and two below the first hole band. These levels can be filled up with one or two holes, respectively. Obviously the polarization of the perturbed spins is much larger in the case of two turned spins and one additional hole than in the case of one turned spin only. Doping a system with two holes and additionally turning two Cu spins leads to a polarization of the perturbed spins comparable to the situation of one flipped spin and one hole. The energy of this two-turned-spin cluster with two holes is at least for larger U the same as for two separated clusters with one turned spin and one hole. In the limit $U \to \infty$ and one additional hole the ground state should be totally ferromagnetically ordered according to Nagaoka's theorem [17].

So far we have confined ourselves to a symmetry breaking solution of the translational invariant three-band Hubbard hamiltonian. However, as in the theory of strong coupling polarons (Pekar-type solutions) one should in principle perform a Bloch-superposition of these wave-functions to guarantee the translational invariance of the solution. This ends up with a dispersion relation for the quasi-particles i.e. in our case the spin-polarized clusters. To keep the calculation tractable we have confined ourselves to hopping processes of a magnetic polaron with one turned spin to nearest and next nearest neighbours. The dispersion relation of the polaron is strongly anisotropic in k-space and yields the maximum of the effective mass in $< 11 >$-direction. For $U = 8T$ and $\epsilon = 3T$ we obtain a value of 10 bare masses.

Table 1. The binding energy and the Cu-spin polarization for the undoped $\langle n_\uparrow \rangle$, $\langle n_\downarrow \rangle$ an doped $\langle n'_\uparrow \rangle$, $\langle n'_\downarrow \rangle$ cases with one and two turned spins in dependence of U and ϵ (Hartree-Fock approach).

$\frac{U}{T}$	$\frac{\epsilon}{T}$	$\langle n_\uparrow^0 \rangle$	$\langle n_\downarrow^0 \rangle$	1 turned spin, 1 hole			2 turned spins, 1 hole			2 turned spins, 2 holes		
				$\langle n'_\uparrow \rangle$	$\langle n'_\downarrow \rangle$	$-\Delta E$	$\langle n'_\uparrow \rangle$	$\langle n'_\downarrow \rangle$	$-\Delta E$	$\langle n'_\uparrow \rangle$	$\langle n'_\downarrow \rangle$	$-\Delta E$
4	2	.66	.03	.31	.57	.12	.12	.65	.04	.32	.55	.38
6	2	.84	.005	.29	.76	.30	.11	.82	.24	.29	.75	.63
8	2	.91	.002	.25	.86	.37	.11	.89	.37	.26	.86	.74
6	3	.77	.008	.25	.68	.22	.10	.75	.11	.25	.67	.51
8	3	.88	.002	.21	.83	.31	.09	.86	.30	.21	.83	.64
10	3	.93	.0008	.18	.90	.34	.08	.92	.37	.18	.90	.68

Table 2. The binding energy and the Cu-spin polarization for the undoped $\langle n_\uparrow \rangle$, $\langle n_\downarrow \rangle$ an doped $\langle n'_\uparrow \rangle$, $\langle n'_\downarrow \rangle$ case with one turned spins in dependence of U and ϵ (Slave-boson approach).

$\frac{U}{T}$	$\frac{\epsilon}{T}$	$\langle n_\uparrow^0 \rangle$	$\langle n_\downarrow^0 \rangle$	1 turned spin, 1 hole		
				$\langle n'_\uparrow \rangle$	$\langle n'_\downarrow \rangle$	$-\Delta E$
6	2	.83	.008	.34	.66	.28
7	2	.88	.004	.35	.71	.36
8	2	.91	.002	.35	.73	.41
6	3	.76	.020	.35	.55	.23
7	3	.84	.006	.34	.64	.30
8	3	.88	.002	.34	.68	.37

3. Slave-boson-approach

In the previous section we have used a selfconsistent Hartree-Fock mean-field approach to determine the polarization and binding energy of the spin-polarized clusters. However, the renormalization of the band widths due to the strong correlation effects in the considered systems is not taken into account by this approach. This effect can be incorporated by using the slave-boson method in the saddle-point approximation, introduced by Kotliar and Ruckenstein [18], which is similar to the Gutzwiler variational approach.

We enlarge the original Hilbert space by introducing four boson fields for every copper site, respectively. $e_i^\dagger$ creates an empty state, $s_{i,\uparrow}$ and $s_{i,\downarrow}$ singly occupied states with spin up and down and finally $d_i^\dagger$ stands for the creation of a doubly occupied state. Since there are only four possible states per Cu site, the unphysical states are eliminated by the following conditions

$$e_i^\dagger e_i + \sum_\sigma s_{i,\sigma}^\dagger s_{i,\sigma} + d_i^\dagger d_i = 1 \tag{28}$$

$$c_{i,\sigma}^{d\dagger} c_{i,\sigma}^{d} - s_{i,\sigma}^\dagger s_{i,\sigma} - d_i^\dagger d_i = 0 \tag{29}$$

where $c_{i,\sigma}^{d\dagger}$ stands for the creation of a hole with spin σ on the Cu site i.

In the saddle-point approximation the constraints (28,29) are only satisfied on the average by the Lagrange parameters λ_σ and κ, respectively.

In analogy to the previous section we double the unit cell by introducing two operators $c_{n,\sigma}^{1d}$ and $c_{n,\sigma}^{2d}$ which create holes with spin σ on the neighbouring Cu sites of the corresponding unit cell n. The symmetry of the AF ordered ground state provides the following relations

$$\lambda_\uparrow^1 = \lambda_\downarrow^2 \tag{30}$$

$$\langle n_{1,\sigma}\rangle = \langle n_{2,-\sigma}\rangle \tag{31}$$

This ends up with the Gutzwiler variational expression for the total energy

$$NE = \sum_\sigma \langle H_\sigma^{eff}\rangle + UNd^2 - N[\lambda_\uparrow\langle n_\uparrow\rangle + \lambda_\downarrow\langle n_\downarrow\rangle] \tag{32}$$

$$H_\sigma^{eff} = \sum_n \epsilon_1 c_{n,\sigma}^{\dagger 1d} c_{n,\sigma}^{1d} + \sum_n \epsilon_2 c_{n,\sigma}^{\dagger 2d} c_{n,\sigma}^{2d} + \sum_m \epsilon_p c_{n,\sigma}^{\dagger p} c_{n,\sigma}^{p} + T_\sigma \sum_{n,m} [c_{n,\sigma}^{\dagger 1d} c_{m,\sigma}^{p} + h.c.] + T_{-\sigma} \sum_{n,m} [c_{n,\sigma}^{\dagger 2d} c_{m,\sigma}^{p} + h.c.] \tag{33}$$

with

$$\epsilon_1 = \epsilon^d + \lambda_\uparrow \tag{34}$$

$$\epsilon_2 = \epsilon^d + \lambda_\downarrow \tag{35}$$

$$T_\sigma = T \frac{\sqrt{(1-\langle n^d\rangle + d^2)(\langle n_\sigma^d\rangle - d^2)} + d\sqrt{\langle n^d\rangle - \langle n_\sigma^d\rangle - d^2}}{\sqrt{\langle n_\sigma^d\rangle(1-\langle n_\sigma^d\rangle)}} \tag{36}$$

The summation in the transfer terms is restricted to nearest neighbours. The diagonalization of (33) can now be performed in the same way as in the first section. The Green's functions keep the same analytical form where additionally the substitution

$$T^2 \rightarrow T_\uparrow T_\downarrow \tag{37}$$

has to be made.

3.1. Doped system

We will add now an additional hole to the system and show that a spin-flip process at site e.g. 0 will lead to a lower ground state energy. Such a spin reversion affects the Lagrange parameters $\lambda_{0,\sigma}$, the double occupancy parameter d_0^2 and additionally the transfer to the next nearest oxygen atoms. Introducing symmetric combinations of these oxygen states the problem reduces to a 2×2 perturbation matrix for each spin direction

$$V_\sigma = \begin{pmatrix} V_\sigma^\lambda & V_\sigma^T \\ V_\sigma^T & 0 \end{pmatrix} \tag{38}$$

in the basis of $|c_{0,\sigma}\rangle$ and $|q\rangle = \frac{1}{2}\sum_{i=1}^4 |p_i\rangle$ where the summation is restricted to the four next nearest oxygen ions of site 0. The perturbations are denoted by

$$V_\sigma^\lambda = \lambda_\sigma^1 - \lambda_\sigma \tag{39}$$

$$V_\sigma^T = 2(T_\sigma^1 - T_\sigma) \tag{40}$$

Following again the Green's functions formalism we can calculate the disturbed Green's functions at the perturbed Cu site from eq.(22).

$$G_{00}^\sigma = \frac{G_{00}^{0,\sigma}}{DET_\sigma(E)} \tag{41}$$

$$DET_\sigma(E) = 1 + \frac{V_\sigma^T}{T_\sigma}\left(1 + \frac{V_\sigma^T}{4T_\sigma}\right) - G_{00}^{0,\sigma}\left[V_\sigma^\lambda + \frac{V_\sigma^T}{T_\sigma}(E-\epsilon_\sigma)\left(1+\frac{V_\sigma^T}{4T_\sigma}\right)\right] \tag{42}$$

Then we have to minimize the change of energy due to the three parameters $\lambda_{0,\uparrow}, \lambda_{0,\downarrow}$ and d_0^2. For every parameter set we have additionally to calculate the new Cu polarization values using eq. (24). As in the first calculation we obtain two localized levels in the CT gap corresponding to the zeros of $DET_\sigma(E)$, one arising from the lower Hubbard band whereas the other comes from the first oxygen type band. Unlike in the first approach these two levels are now both located in the upper region of the CT gap and only separated by ≈ 0.2 eV. The level below the lower Hubbard band is localized very near the band edge and disappears for larger values of U.

Table (2) shows the results obtained for various values of U and $\epsilon = E_p - Ed$. As one can readily see, the incorporation of fluctuations within the scope of a slave-boson approximation reduces the polarization of the spin-cluster state to $10-20\%$ in comparison to the Hartree-Fock approach. On the other hand we now obtain a larger value of the binding energy.

4. Percolation Thresholds

The hole-clusters are practically immobile due to the small probability of spin-flip processes which have to accopmpany the motion of the clusters. On increasing the concentration of the holes, and with it that of the immobile clusters, at a critical concentration $c_{crit.}$ the clusters build up a percolation network along the lines of which the holes can move freely, and the system goes from the insulating to the conducting state [6, 5]. Within the percolation model the magnetic properties of the perovskite-type materials can be understood by taking the three-dimensional magnetic ordering into account which is characterized by strong in-plane and weak inter-plane interactions. Three different percolation thresholds are obtained [5]:

1. Percolation lines in the plane are built up from clusters of both spin directions. This limit characterizes the destruction of long-range AF order caused by the strong in-plane magnetic interactions and corresponds to a hole concentration

$$c_M^{(1)} \approx \frac{2.2}{8N} \tag{43}$$

where N denotes the number of parallel aligned Cu-spins per cluster.

2 Percolation lines in the planes are built up from clusters with the same spin orientation. This limit is important for the motion of the charge carriers and characterizes the transition to electrical conductivity corresponding to a hole concentration

$$c_c \approx \frac{4.4}{7N} \tag{44}$$

3 At higher concentrations the three-dimensional inter-plane percolation of AF-ordered areas will be destroyed. At this second magnetic threshold the system finally loses also the weak long-range AF order

$$c_M^{(2)} \approx \frac{15.8}{18N} \tag{45}$$

These considerations lead to the following relation between the three critical concentrations:

$$c_M^{(1)} \geq 1.4 c_c \approx 3.2 c_M^{(2)} \tag{46}$$

For $La_{2-x}(Sr,Ba)_xCuO_4$, where the hole concentration c equals 2x, this leads to $x_M^{(1)} \approx 0.02, x_c \approx 0.05, x_M^{(2)} > 0.08$ in agreement with experiment [19]. In the case of $YBa_2Cu_3O_{6+x}$ a phase transition from tetragonal to orthorombic structure appears at $x \approx 0.4$ connected with the ordering of oxygens in the chains. This leads to the fact that for $x < 0.4$ most of the holes are kept in the chains, whereas at $x \approx 0.4$ a large number of holes are introduced into the planes, bringing the system immediately above the threshold for destruction of strong AF order and the beginning of electrical conductivity.

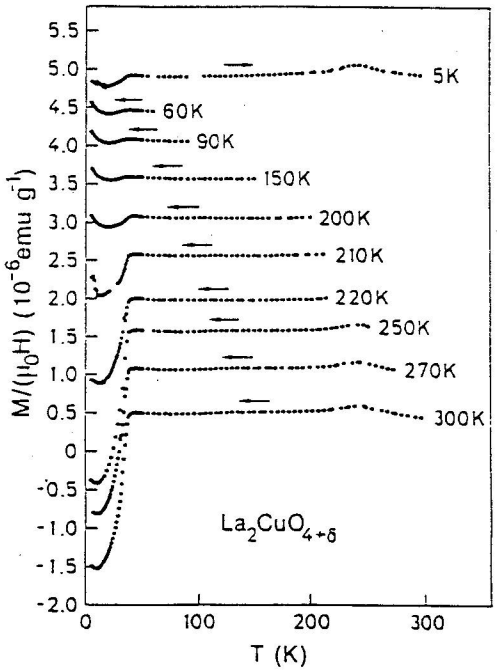

Fig. 2. Magnetization of a $La_2CuO_{4+\delta}$ sample as a function of temperature. The starting temperatures T_S to which the sample was quenched from room temperature are indicated. The uppermost curve was obtained after quenching the sample to 5K and slowly heating to room temperature. Beginning from the lowest data set each curve was shifted upwards by a value of 5×10^7 emu g^{-1} compared to the preceeding one. The measuring field was 90 G, arrows indicate the direction of temperature change during the measurements.

5. Experimental evidence for percolative phase separation

Field dependent magnetization measurements in slightly doped (oxygen enriched as well as Sr doped) La_2CuO_4 samples show the formation of conducting phases by the existence of a percolative phase separation [1].The essential results are summarized in fig.(2). Below 37 K, the sample of $La_2CuO_{4+\delta}$ exhibits a sharp transition from the paramagnetic to a diamagnetic magnetization indicating the presence of superconductivity. The diamagnetic fraction in the magnetization strongly depends on the temperature T_S to which the sample was rapidly quenched. Below T_S magnetization data were acquired

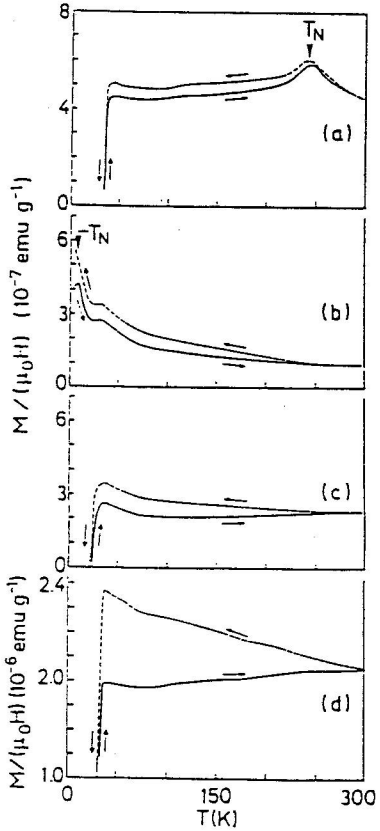

Fig. 3. fc and zfc magnetization of the $LaCuO_{4+\delta}$ sample and moderately Sr doped samples $La_{2-x}Sr_xCuO_4$ as a function of temperature. Arrows indicate the direction of the temperature variation. The zfc magnetization curve was measured after the sample had been cooled slowly from room temperature to 5K by using the same temperature interval step sequence, including equilibriation as in the subsequent heating (or cooling) cycles and with applied magnetic field. The Neel temperature T_N for the $La_2CuO_{4+\delta}$ samples and for $La_{1.94}Sr_{0.06}CuO_4$ are indicated. Note: the zero of ordinate for $La_{1.94}Sr_{0.06}CuO_4$ has been suppressed.

during slow cooling temperature scans. Note that a sudden decrease of the diamagnetic fraction occurs at values of T_S in the range of 200-250 K. Surprisingly, the same sample quenched to 5 K (fig.(2), uppermost curve) shows a very small diamagnetic fraction only. This clearly proves that superconductivity can almost completely be suppressed by rapid temperature quenching of the sample. If, however, cooling was performed slowly the diamagnetic shielding signal became maximal. As shown in [1] the formation of superconducting phases can also be initiated by application of sizeable magnetic fields. The results obtained for the Sr doped samples can be seen in fig.(3) showing an increasing diamagnetic fraction with higher Sr contents. The most obvious feature is the distinct separation between the field cooled (applied measuring field of 90G) and the zero-field cooled magnetization both for the $La_2CuO_{4+\delta}$ and the Sr doped samples in

the same temperature range. It is important to note that this temperature range is well above any of the Neel temperatures in the Sr doped samples. We find that the $La_2CuO_{4+\delta}$ sample shows quantitatively similar behaviour as the $La_{1.98}Sr_{0.02}CuO_4$ sample. All these measurements clearly prove that in the investigated $La_2CuO_{4+\delta}$ samples diffusion processes of magnetic quasi particles take place which can be influenced either by thermal treatment (fast and slow cooling) or by magnetic fields. Not all the quasiparticles, however, contribute to the conducting phase which is of fractal nature but rather coexist with single magnetic quasiparticles which give rise to the observed paramagnetic behaviour. The equilibrium between these two subsystems can be shifted by thermal treatment of the samples. This coexistence and the by thermal treatment activated redistribution effects can clearly be observed in $La(Sr)CuO_4$ samples too. With increasing temperature thermal fluctuations gradually destroy the conducting (superconducting) phase breaking it up into magnetic quasiparticles as can be seen by the monotonic increase in the paramagnetic signal (fig.(3) c and d, lower curves).

6. Conclusion

We showed that in the discussed MF approximations of the three band Hubbard model doping with holes leads to the creation of ferromagnetically ordered clusters. This process is more pronounced when taking the influence of dopant ions (e.g. Sr, Ba, O etc.) into account. The occuring attractive interaction between these charge compensators and the holes in addition supports the hole-localization. The size of the clusters depends on the Coulomb repulsion on the Cu sites. Doping of the CuO_2 planes leads to a separation of the system into hole rich spin clusters (ferrons) and hole free AF ordered regions. The metal insulator transition (MIT) is provided by the percolation of clusters with the same spin direction. However, in the vicinity of the MIT there still exists long range AF order in regions between the percolation lines in accordance with experiment.

References

[1] R.K.Kremer,E.Sigmund,V.Hizhnyakov,F.Hentsch,A.Simon, K.A.Müller,M.Mehring,*Z.Phys.B Cond.Matter* **86**, (1992) 319

[2] P.C.Hammel,A.P.Reyes,Z.Fisk,M.Takigawa,J.D.Thompson, K.H.Heffner,S.W.Cheong, *Phys.Rev.* B**42**, 1990) 6781

[3] J.D.Jorgensen,B.Dabrowski,Pei Shiyou, D.G.Hinks,L.Soderholm,B.Morosin,J.E.Schirber, E.L.Venturini,D.S.Ginley,*Phys.Rev.* B**38**, (1988) 11337

[4] C.Chaillout, S.W.Cheong,Z.Fisk,M.S.Lehmann,M.Marezio, B.Morosin, J.E.Schirber, *Physica* C**158**, (1989) 183

[5] V.Hizhnyakov, E.Sigmund, *Physica* C**156**,(1988) 655

[6] V.Hizhnyakov, E.Sigmund, M.Schneider,*Phys.Rev.* B**44**, (1991) 795

[7] C.Taliani,A.Pal,G.Ruani,R.Zamboni,X.Wei and Z.V.Vardeny in *Electronic Properties of High* **Tc** *Superconductors and Related Compounds* ed. by H.Kuzmany,M.Mehring and J.Fink, Springer Series on Solid State Science, Berlin 1990

[8] G.Wübbeler,O.Schirmer,*Phys.Stat.Sol* B**174**, (1992) K21

[9] J.Mesot,P.Allenspach,U.Staub,A.Furrer,H.Mutka, *Phys.Rev.Lett.* **70** (1993) 865

[10] P.G.Baranov,A.G.Badalyan, *Solid State Commun.* **85**, (1993) 987
[11] G.Benedeck,K.A.Müller (eds.),*Proceedings of the ERICE-Workshop on Phase Separation in Cuprate Superconductors*, World Scientific (Singapore),May 1992
[12] E.Sigmund,K.A.Müller (eds.),*Proceedings of the COTTBUS-Workshop on Phase Separation in Cuprate Superconductors*, Springer,1994
[13] V.J.Emery,*Phys.Rev.Lett.* **58**, (1987) 2794
[14] E.N.Economou,*Green's Functions in Quantum Physics*, Springer Verlag (1990)
[15] A.M.Oleś,J.Zaanen,*Phys.Rev.* B**39**,(1989) 9175
[16] A.Auerbach,B.E.Larson,*Phys.Rev.Lett.* **66** (1991) 2262
[17] Y.Nagaoka,*Phys.Rev.* B**147**,(1966) 392
[18] G.Kotliar,A.Ruckenstein,*Phys.Rev.* B**57**, (1986) 1362
[19] A.Weidinger,C.Niederring,A.Golnik,R.Simon, E.Recknagel,*Phys.Rev.Lett.***62**,(1989) 102